



# Investigating the Complex Permittivity of Low Voltage Power Cables Under Different Stresses

Ramy S. A. Afia<sup>1,2(✉)</sup>, Ehtasham Mustafa<sup>2,3</sup>, Semih Bal<sup>2</sup>,  
and Zoltán Ádám Tamus<sup>2</sup>

<sup>1</sup> Department of Electrical Power and Machines Engineering, Faculty of Engineering, Helwan University, Cairo, Egypt  
ramysaad@h-eng.helwan.edu.eg

<sup>2</sup> Department of Electric Power Engineering, Faculty of Electrical Engineering and Informatics, Budapest University of Technology and Economics, Budapest, Hungary

{mustafa.ehtasham,bal.semih,tamus.adam}@vet.bme.hu

<sup>3</sup> Department of Electrical Engineering, Faculty of Engineering and Technology, Gomal University, Dera Ismail Khan, Pakistan

**Abstract.** This paper presents results of electrical tests carried out on nuclear power plant low voltage power cable samples based XLPE/CSPE polymer insulation. These cable samples have been subjected to accelerated thermal and mechanical stresses for 240, 480, 720 and 960 h. The effect of these aging stresses has been investigated through studying the real and imaginary parts of complex permittivity over frequency range from 20 Hz to 500 kHz. These two parameters are commonly used as aging markers to assess the insulation state of such kind of cables. The results show a non-uniform trend for the real and imaginary parts of permittivity. Also, it can be noticed that after the last two cycles, the imaginary part minimum values have been shifted to lower frequencies, 200 Hz.

**Keywords:** Nuclear power plant cables · Low voltage power cables · Aging stresses · Complex permittivity · Condition monitoring

## 1 Introduction

The continuous operation of Nuclear Power Plants (NPPs) relies on many components. One of these components is an enormous amount of cable systems. A typical nuclear power plant may compose of 1000 to 2000 km of cables. These cables are classified as Low Voltage (LV) & Medium Voltage (MV) Power cables, Instrumentation and Control (I&C) cables, special cables and general service cables [1–4]. These cables provide the communication between equipment, control and safety systems which monitor these plants. The insulation of these cables is mostly based on polymeric materials such as Cross-Linked Polyethylene (XLPE), Ethylene Propylene Rubber (EPR), Ethylene Vinyl Acetate (EVA), Polyether Ether Ketone (PEEK) and Cross-Linked Polyolefin (XLPO) [4, 5]. Different ageing mechanisms affect the polymeric insulation of such cables, multi-stress aging [6, 7]. As a results, the functionality of

these cables is not ensured under the effect of these ageing mechanisms. However, the functionality of NPP cables should be guaranteed during the normal operation and during the Design Basis Event (DBE) [8, 9]. Multiple cable testing techniques have been widely developed for investigating the aging process of NPP cables [10]. The insulation state and role of low voltage power cables in nuclear power plants are frequently monitored through a destructive test technique. This testing technique named Elongation at Break (EaB) [11]. The advantage of this test is that, the aging can be effectively correlated but on the other hand, it requires sample scarification to be investigated and a proper laboratory is needed [3]. For lifetime extension, the cables must undergo a non-destructive test technique where some aging markers can be measured in-situ. Recently, measuring the electrical parameters of LV NPP cables became a trend of many researchers. For instance, measuring the capacitance, loss factor, impedance, insulation resistance and complex permittivity. A significant change in the electrical parameters of LV cables has been observed with aging. This paper presents a Frequency Domain Spectroscopy (FDS) of XLPE/CSPE insulation-based LV NPP power cable samples. The samples have been subjected to a sequential thermal and mechanical stresses. The study was based on the measurement of real ( $\epsilon'$ ) and imaginary ( $\epsilon''$ ) parts of permittivity. The real part represents the stored energy in the material when it is exposed to electric field while  $\epsilon''$  influence the energy absorption and attenuation. A high precision impedance analyser with frequency spanning from 20 Hz to 500 kHz has been used for the measurement of  $\epsilon'$  and  $\epsilon''$ .

## 2 Relationship to Life Improvement

Energy makes marvelous things happen and its capacity to produce bright, radiant light makes an especially striking impression when it arrives. Electricity's introduction thus tends to be associated with progress and modernity. Electricity make big difference in many obvious places such as our homes, food, the commercial and manufacturing sectors, communication and transportation, entertainment, easier education and better health care. This makes the industry of electric power to have the large investments. Nuclear power plants are of the strategic ways to generate energy with many advantages like relatively low costs, providing a stable base load of energy and low pollution. In contrast, in case of accidents, radioactive waste possesses a threat to the environment and it is very dangerous for human beings. Because of the importance of the nuclear power plant cables, they must undergo a qualification process to ensure that these cables will do they intended functions. In addition, for lifetime extension, this qualification process has to be done in a non-destructive way since the replacement cost of these cables is not affordable. The harsh operating conditions in nuclear power plants accelerates the aging processes of cables causing failure. It is important to state the insulation state of these cables before insulation damage and this is a great challenge since there are many factors may cause this. Accelerated aging tests are required to examine the impact of different aging mechanism on insulation integrity of such kind of cables. So, in this paper, low voltage power cable samples used in nuclear power plants have been investigated to study the effect of thermal and mechanical stresses. The study based on frequency domain spectroscopy using impedance analyser over a wide

frequency range. The two parts of complex permittivity, real and imaginary parts have been studied.

### 3 Experimental Work

#### 3.1 Specimens

Low voltage (600 V) NPP power cable samples have been investigated. As shown in Fig. 1, the cable comprises three parts, tin-coated copper conductor, XLPE inner insulation and CSPE outer jacket. Table 1 lists the cable specifications.



Fig. 1. Cable construction

#### 3.2 Experimental Setup and Dielectric Measurements

Impedance analyzer has been used to measure the dielectric parameters over a range of frequency from 20 Hz to 500 kHz at 5 V<sub>rms</sub> output voltage. Based on the measured parameters, the real and imaginary parts of the complex permittivity have been calculated using Eqs. (1) and (2). As shown in Fig. 2b, the measurement was executed in Faraday cage to reduce the electromagnetic interferences. The test temperature was 25 °C ± 2%.

$$\varepsilon' = \frac{dC}{A\varepsilon_o} \quad (1)$$

$$\varepsilon'' = \frac{d}{AR\omega\varepsilon_o} \quad (2)$$

Where  $A$  and  $d$  are the electrode area and thickness of insulation respectively. The vacuum permittivity is given as  $\varepsilon_o$  ( $\varepsilon_o = 8.85419 \times 10^{-12}$  F/m) and  $\omega$  is the angular frequency ( $\omega = 2\pi f$ ),  $f$  is the frequency expressed in Hz.  $R$  is resistance measured in ohm ( $\Omega$ ).

**Table 1.** Cable specifications.

Parameter	Value
Nominal voltage	0.6 kV
Inner insulation	XLPE
Insulation thickness	1.143 mm
Jacket material	CSPE
Jacket thickness	0.762 mm
Continuous bending radius	38.1 mm
Overall diameter	8.636 mm

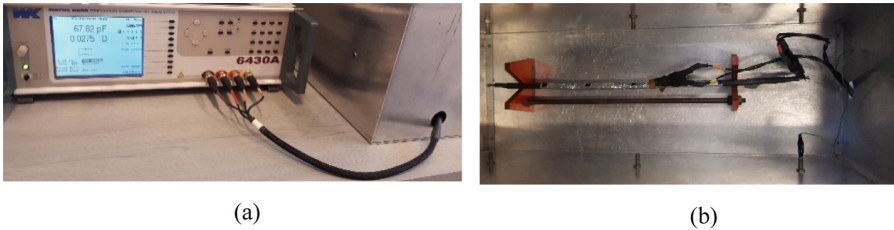


**Fig. 2.** Measurement setup (a) Impedance analyzer (b) Test sample connected to the measuring clamps in Faraday cage

### 3.3 Accelerated Aging Procedure

Two aging mechanisms have been applied to all samples. 4 aging cycles, the first and third are thermal aging cycles while the second and fourth are mechanical aging cycles. The thermal aging cycles are indexed as 1T, 2T while 1M, 2M for the mechanical aging cycles. The period of each cycle is 240 h. The thermal aging has been done by placing the samples in an oxygen-controlled oven at temperature 120 °C. After each thermal cycle and before starting the measurements, the samples left for one day at room temperature. For mechanical aging, the samples have been spiraled on a cylinder of 4.5 cm diameter.

## 4 Experimental Results

The behavior of the real part ( $\epsilon'$ ) of the complex permittivity is illustrated in Fig. 3. Regardless the aging type, the  $\epsilon'$  increased as the frequency stepped down. With the end of thermal cycle 1T,  $\epsilon'$  has increased over the whole frequency range. After the first mechanical cycle, 1M and the second thermal cycle, 2T, a reduction in  $\epsilon'$  has been observed for all frequencies. But after the second mechanical cycle, 2M, the  $\epsilon'$  has increased again over frequency range from 20 Hz to 250 kHz and slightly declined at frequencies 300 and 400 kHz.

Moving to the imaginary part ( $\epsilon''$ ) of the complex permittivity, the plot of  $\epsilon''$  as a function of frequency is shown in Fig. 4.  $\epsilon''$  is plotted for frequencies from 200 Hz to

500 kHz as the resistance value at the frequencies below 200 Hz it greater than the maximum measuring range of the used device. As shown in Fig. 4, the  $\epsilon''$  increased as the frequency increased independent of the aging type. After thermal cycle 1T, the  $\epsilon''$  has increased over frequencies ranged from 20 Hz to 250 kHz while it decreased over frequencies 300, 400 and 500 kHz. At the end of the first mechanical cycle, 1M, the  $\epsilon''$  has increased from 200 Hz to 10 kHz while it decreased for the other frequencies up to 500 kHz. Also, the  $\epsilon''$  has decreased after the second thermal cycle, 2T over the entire frequency range. After the last cycle, 2M, the  $\epsilon''$  increased over all frequencies in comparison with the second thermal cycle, 2M.

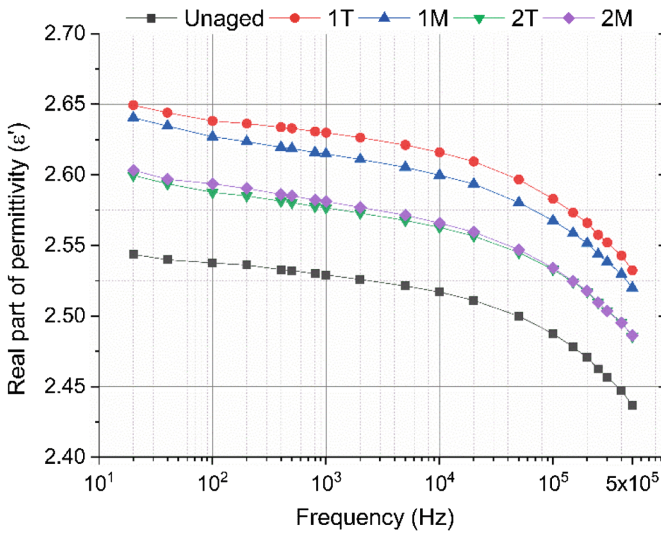


Fig. 3. Real part of permittivity versus frequency

To understand the changing behavior of  $\epsilon''$ , frequencies 500 Hz, 1 kHz, 20 kHz and 50 kHz have been chosen as reference. As can be seen in Fig. 5, at frequencies 500 Hz and 1 kHz, an increment in  $\epsilon''$  has been observed after the first and second aging cycles then it declined after the third cycle and raised after the fourth cycle. While at frequencies 20 kHz and 50 kHz,  $\epsilon''$  went up after cycles 1T and 2M but dropped after 1M and 2T cycles (Fig. 5).

## 5 Discussion

Since the real part of permittivity,  $\epsilon'$  is related to the polarization phenomena and as the insulating materials are polar in nature. The considerable increment in  $\epsilon'$  after the first thermal cycle suggests an increase in the polarization process where chemical bonds were broken resulting in generation of dipoles and presenting micro voids between inner insulation and outer jacket which are source of space charges. The reduction in  $\epsilon'$

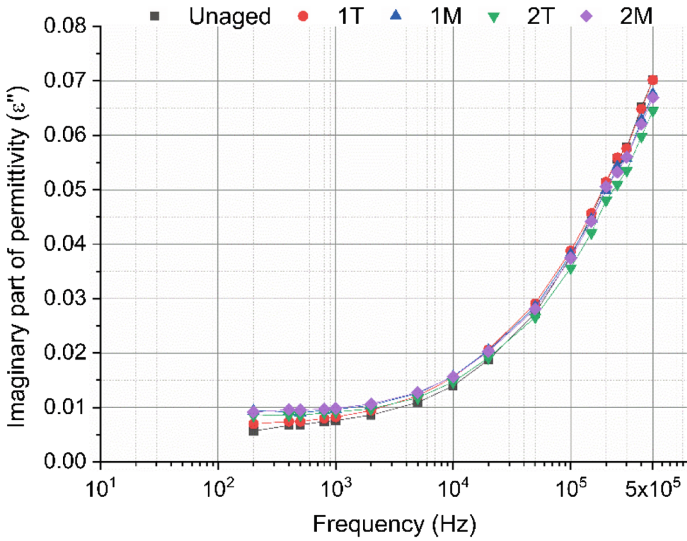


Fig. 4. Imaginary part of permittivity versus frequency

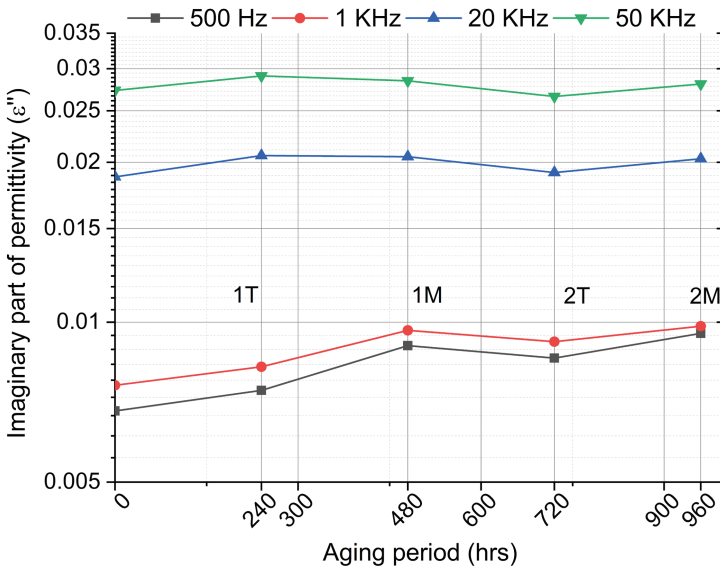


Fig. 5. Behaviour of imaginary part of permittivity at 500 Hz, 1 kHz, 20 kHz and 50 kHz

after the mechanical cycle, 1M, due to the mechanical stress, the micro voids which have been created after the first cycle have been reduced due to the compressive nature of the mechanical stress thus the polarization has decreased. With increasing the aging period, more structural changes happened to the insulation leading to reduction in the

dipoles thus  $\epsilon'$  has decreased but after the second mechanical cycle, a noticeable increase in  $\epsilon'$  suggest the presence of micro cracks which associated with polymer materials under mechanical stress as reported in [12]. These micro cracks behave the same as the micro voids and hence add to the polarization.

The imaginary part of permittivity,  $\epsilon''$  is related to energy loss or insulation conductivity. The increment of  $\epsilon''$  after the first cycle, 1T is an indication for the presence of charge carriers produced due to structural changes also the presence of micro voids which contribute to the conduction process. The increase of  $\epsilon''$  after the first mechanical cycle shows the presence of chemical species which are contributing to the conduction losses in spite of the reduction in micro voids. After cycle 2T, the chemical species adding to the conduction losses have decreased due to re-creation of new bonds and hence resulted in reduction of  $\epsilon''$ . As mention for  $\epsilon'$  after the second mechanical cycle, the space charges due to the presence of micro cracks are also added to the conduction losses.

Shifting the minimum values of  $\epsilon''$  to lower frequencies is plotted in Fig. 6. This shows that the polar or ionic particles have decreased while it contributes the conduction process.

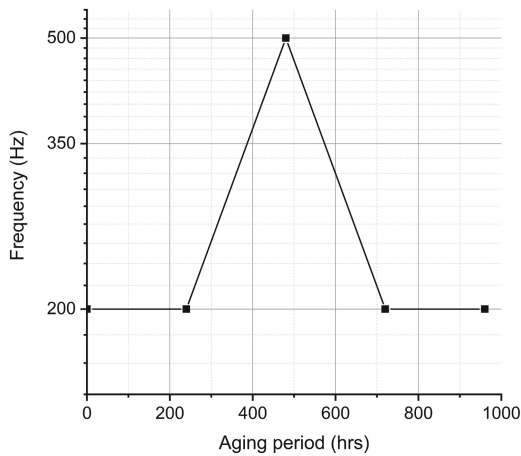


**Fig. 6.** Shifting the minimum values of  $\epsilon''$  versus the aging period

It should be noted that, during the manufacturing process of insulating materials, some additives are added to provide a special properties such as flame retardants, antioxidants. These additives affect the structural changes of insulating materials during aging processes. Chemical investigations such as OIT, DSC and TGA will provide a clear understanding for the effect of aging stresses [13].

## 6 Conclusion

The complex permittivity of low voltage insulation based XLPE/CSPE power cables has been studied in this research. The samples have been subjected to sequential thermal and mechanical stresses for four aging cycles each spanned to 10 days. The thermal stress carried out at temperature 120 °C and the mechanical stress carried out by spiraling the samples over a cylinder with a diameter of approx. 5% higher than the cable diameter. The results reported in this work shows that the polarization and conduction processes which are related to the real,  $\epsilon'$  and imaginary,  $\epsilon''$  parts of permittivity are affected with the thermal and mechanical aging mechanisms. Both,  $\epsilon'$  and  $\epsilon''$  have increased after the first thermal cycle and decreased after the second thermal cycle. For mechanical aging cycles, 1M and 2M,  $\epsilon'$  increased after 1M and decreased after 2M while  $\epsilon''$  has increased after both cycles. Only after 1M,  $\epsilon''$  has increased over frequency range 200 Hz to 10 kHz.

**Acknowledgments.** This research work has been implemented under Project No. 123672 with the support provided from the National Research, Development and Innovation Fund of Hungary, financed under the KNN\_16 funding scheme.

## References

1. Mustafa, E., Ádám, T.Z., Afia, R.S.A., Asipuella, A.: Thermal degradation and condition monitoring of low voltage power cables in nuclear power industry. In: Camarinha-Matos, Luis M., Almeida, R., Oliveira, J. (eds.) DoCEIS 2019. IAICT, vol. 553, pp. 405–413. Springer, Cham (2019). [https://doi.org/10.1007/978-3-030-17771-3\\_35](https://doi.org/10.1007/978-3-030-17771-3_35)
2. Asipuella, A., Mustafa, E., Afia, R.S.A., Ádám, T.Z., Khan, M.Y.A.: Electrical condition monitoring of low voltage nuclear power plant cables:  $\tan\delta$  and capacitance. In: 2018 International Conference on Power Generation Systems and Renewable Energy Technologies (PGSRET), pp. 1–4. IEEE (2019)
3. Verrardi, L., Fabiani, D., Montanari, G.C., Gedde, U.W., Linde, E.: Aging investigation of low-voltage cable insulation used in nuclear power plants, pp. 851–854 (2012)
4. Afia, R.S.A., Ádám, T.Z., Mustafa, E.: Effect of combined stresses on the electrical properties of low voltage nuclear power plant cables. In: Camarinha-Matos, Luis M., Almeida, R., Oliveira, J. (eds.) DoCEIS 2019. IAICT, vol. 553, pp. 395–404. Springer, Cham (2019). [https://doi.org/10.1007/978-3-030-17771-3\\_34](https://doi.org/10.1007/978-3-030-17771-3_34)
5. Lee, S.H., Lee, J.D., Kim, M.Y., Jang, H.S., Jeong, C.H.: Evaluation of accelerated ageing cables used in nuclear power plant. In: Proceedings of 2012 IEEE International Conference on Condition Monitoring and Diagnosis, pp. 681–684 (2012)
6. Afia, R.S.A., Mustafa, E., Ádám, T.Z.: Mechanical stresses on polymer insulation materials. In: IEEE International Conference on Diagnostics in Electrical Engineering, pp. 2–5 (2018)
7. Mustafa, E., Afia, R.S.A., Tamus, Z.Á.: Condition monitoring uncertainties and thermal - radiation multistress accelerated aging tests for nuclear power plant cables: a review, 1–13 (2019)
8. Glass, S.W., et al.: Assessment of NDE for key indicators of aging cables in nuclear power plants - interim status. In: AIP Conference Proceedings, vol. 1706 (2016)

9. Anandakumaran, K., Seidl, W., Castaldo, P.V.: Condition assessment of cable insulation systems in operating nuclear power plants. *IEEE Trans. Dielectr. Electr. Insul.* **6**, 376–384 (1999)
10. Series, I.T.: Benchmark analysis for condition monitoring test techniques of aged low voltage cables in nuclear power plants. IAEA-TECDOC-1825, p. 179 (2017)
11. Banford, M., Fouracre, R.A.: Nuclear technology and ageing. *IEEE Electr. Insul. Mag.* **15**, 19–27 (1999)
12. Plaček, V., Kohout, T., Kábrt, J., Jiran, J.: The influence of mechanical stress on cable service life-time. *Polym. Test.* **30**, 709–715 (2011)
13. Mustafa, E., Afia, R.S.A., Tamus, Z.Á.: Investigation of complex permittivity of XLPO insulated photovoltaic DC cables due to thermal aging. In: Németh, B. (ed.) *ISH 2019. LNEE*, vol. 598, pp. 261–269. Springer, Cham (2020). [https://doi.org/10.1007/978-3-030-31676-1\\_25](https://doi.org/10.1007/978-3-030-31676-1_25)